A Molecular Mechanics (MM3(96)) Force Field for Metal−Amide Complexes

Benjamin P. Hay,* Omoshile Clement, Giovanni Sandrone, and David A. Dixon

Theory, Modeling, and Simulation Group, Environmental Molecular Sciences Laboratory, Pacific Northwest National Laboratory, P.O. Box 999, Richland, Washington 99352

Received June 9, 1998

A molecular mechanics (MM3(96)) force field is reported for modeling metal complexes of amides in which the amide is coordinated through oxygen. This model uses a "points-on-a-sphere" approach which involves the parametrization of the M−O stretch, the M−O═C bend, and the M−O═C−X (X = C, H, N) torsion interactions. Relationships between force field parameters and metal ion properties (charge, ionic radius, and electronegativity) are presented that allow the application of this model to a wide range of metal ions. The model satisfactorily reproduces the structures of over fifty amide complexes with the alkaline earths, transition metals, lanthanides, and actinides.

I. Introduction

The need to separate actinide metal ions from nuclear wastes has motivated research to discover organic ligands that can be used for this purpose.[1] Diamide ligands, first examined by Siddell in the 1960s,[2] have been extensively investigated for their application as f-block metal ion sequestering agents.[3] These studies have demonstrated that simple modifications to diamide structure can have a large influence on the performance of the ligand. Yet, despite the amount of research that has been done on these systems, the influence of diamide structure on ligand performance remains poorly understood. This lack of understanding is due, in part, to difficulties in identifying to what extent changes in metal extraction are caused by changes in solubilities, electronic factors, and steric factors.

Our research focuses on interpreting the role of ligand steric factors in these systems and the development of criteria to allow the design of multidentate amides with enhanced metal ion affinity and selectivity. An initial step toward this goal is to identify the geometric preferences of the coordinated amide oxygen donor group. Prior work has demonstrated the importance of ligand donor orientation in defining the complementarity of an array of ligand donor atoms. Knowledge of the specific geometric preferences of the nitrogen donor in metal−amine complexes[4] and the oxygen donor in metal−ether complexes[5,6] was key to understanding the role of ligand architecture on metal complex stability.[6−10] To gain a similar knowledge for the amide oxygen donor, we have reviewed the structural features of monodentate amide ligands in a variety of metal complexes.[11] This survey established the existence of preferred M−O═C angles and M−O═C−X dihedral angles.

The aim of the current study is to incorporate the qualitative observations from the structural review into the quantitative framework of a molecular mechanics model. Molecular mechanics models provide a valuable tool for studying the nature and magnitude of steric interactions in metal complexes.[12−20] A method for the application and interpretation of molecular mechanics calculations has been developed to assess the

* To whom correspondence may be addressed. E-mail: ben.hay@pnl.gov.

(1) (a) Choppin, G. R.; Nash, K. L. *Radiochim. Acta* **1995**, *70*, 225−236. (b) Nash, K. L.; Choppin, G. R. *Sep. Sci. Technol.* **1997**, *32*, 255−274. (c) O'Boyle, N. C.; Nicholson, G. P.; Piper, T. J.; Taylor, D. M.; Williams, D. R.; Williams, G. *Appl. Radiat. Isot.* **1997**, *48*, 183−200.

(2) (a) Siddell, T. H., III. *J. Inorg. Nucl. Chem.* **1963**, *29*, 883−892. (b) Siddell, T. H., III. *J. Inorg. Nucl. Chem.* **1967**, *29*, 149−158. (c) Siddell, T. H., III; Good, M. L.; Whilhite, R. N. *Spectrochim. Acta* **1967**, *23A*, 1161−1164.

(3) (a) Musikas, C. *Inorg. Chim. Acta* **1987**, *140*, 197−206. (b) Musikas, C.; Hubert, H. *Solv. Extr. Ion Exch.* **1987**, *5*, 977−893. (c) Musikas, C. *Sep. Sci. Technol.* **1988**, *23*, 1211−1226. (d) Thiollet, G.; Musikas, C. *Solv. Extr. Ion Exch.* **1989**, *7*, 813−827. (e) Charbonnel, M. C.; Musikas, C. *Solv. Extr. Ion Exch.* **1989**, *7*, 1007−1025. (f) Musikas, C.; Condamines, N.; Cuillerdier, C. *Anal. Sci.* **1991**, *7*, 11−16. (g) Cuillerdier, C.; Musikas, C.; Hoel, P.; Nigond, L.; Vitart, X. *Sep. Sci. Technol.* **1991**, *26*, 1229−1244. (h) Cuillerdier, C.; Musikas, C.; Nigond, L. *Sep. Sci. Technol.* **1993**, *28*, 155−175. (i) Nair, G. M.; Prabhu, D. R.; Mahajan, G. H.; Shukla, J. P. *Solv. Extr. Ion Exch.* **1993**, *11*, 831−847. (j) Nair, G. M.; Mahajan, G. R.; Prabhu, D. R. *J. Radioanal. Nucl. Chem.* **1995**, *191*, 323−330. (k) Tian, Q.; Hughes, M. A. *Hydrometallurgy* **1994**, *36*, 79−94. (l) Nakamura, T.; Miyake, C. *Solv. Extr. Ion Exch.* **1995**, *13*, 253−273. (m) Ruikar, P. B.; Nagar, M. S.; Subramanian, M. S.; Gupta, K. K.; Varadarajan, N.; Singh, R. K. *J. Radioanal. Nucl. Chem., Lett.* **1995**, *201*, 125−134. (n) Sasaki, Y.; Choppin, G. *J. Radioanal. Nucl. Chem.* **1996**, *207*, 383−394. (o) Wang, Y.-S.; Shen, C.-H.; Yang, Y.-H.; Zhu, J.-K.; Bao, B.-R. *J. Radioanal. Nucl. Chem., Lett.* **1996**, *213*, 199−205. (p) Wang, Y.-S.; Sun, G.-X.; Xie, D.-F.; Bao, B.-R.; Cao, W.-G. *J. Radioanal. Nucl. Chem., Lett.* **1996**, *214*, 67−76. (q) Shen, C.; Bao, B.; Zhu, J.; Wang, Y.; Cao, Z. *J. Radioanal. Nucl. Chem., Lett.* **1996**, *212*, 187−196. (r) Chan, G. Y. S.; Drew, M. G. B.; Hudson, M. J.; Iveson, P. B.; Lijenzin, J.-O.; Skalberg, M.; Spjuth, L.; Madic, C. *J. Chem. Soc., Dalton Trans.* **1997**, 649−660. (s) Spjuth, L.; Liljenzin, J. O.; Skalberg, M.; Hudson, M. J.; Chan, G. Y. S.; Drew, M. G. B.; Feaviour, M.; Iveson, P. B.; Madic, C. *Radiochim. Acta* **1997**, *78*, 39−46.

(4) (a) Hancock, R. D. *J. Chem. Educ.* **1992**, *69*, 615−621. (b) Hancock, R. D. *Acc. Chem. Res.* **1990**, *23*, 253−257. (c) Hancock, R. D.; Wade, P. W.; Ngwenya, M. P.; Sousa, A. S. D.; Damu, K. V. *Inorg. Chem.* **1990**, *29*, 1968−1974.

(5) Hay, B. P.; Rustad, J. R.; Hostetler, C. J. *J. Am. Chem. Soc.* **1993**, *115*, 11158−11164.

(6) Hay, B. P.; Rustad, J. R. *J. Am. Chem. Soc.* **1994**, *116*, 6316−6326.

(7) Martell, A. E.; Hancock, R. D. *Metal Complexes in Aqueous Solution*; Plenum Press: New York, 1996.

(8) Martell, A. E.; Hancock, R. D.; Motekaitis, R. J. *Coord. Chem. Rev.* **1994**, *133*, 39−65.

(9) Hay, B. P.; Zhang, D.; Rustad, J. R. *Inorg. Chem.* **1996**, *35*, 2650−2658.

(10) Hay, B. P.; Rustad, J. R. *Supramol. Chem.* **1996**, *6*, 383−390.

(11) Clement, O.; Rapko, B. M.; Hay, B. P. *Coord. Chem. Rev.* **1998**, in press.

(12) Brubaker, G. R.; Johnson, D. W. *Coord. Chem. Rev.* **1984**, *53*, 1−36.

(13) Hancock, R. D. *Prog. Inorg. Chem.* **1989**, *37*, 188−286.

(14) Comba, P. *Coord. Chem. Rev.* **1993**, *123*, 1−48.

10.1021/ic980641j CCC: $15.00
Published on Web 10/07/1998

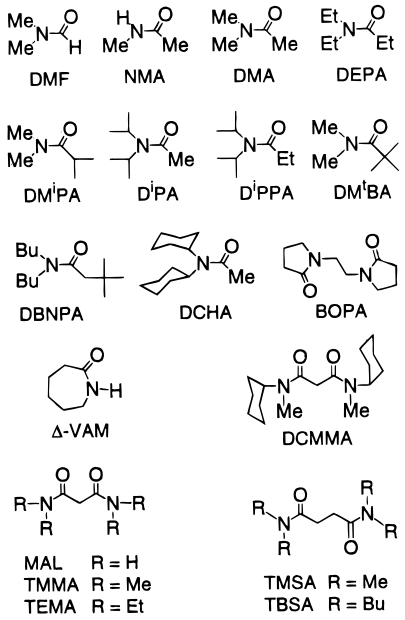

Figure 1. Amide ligands in complexes **1**−**52**.

influence of donor group connectivity on metal ion binding affinity.[9,21] This method uses molecular mechanics strain energies to measure the cost of ligand conformational reorganization and to quantify the degree of complementarity, i.e., how well the donor groups "fit" the stereochemical and geometric requirements of the metal. The application of this approach to multidentate amide ligands requires force field parameters for metal−amide complexes.

Herein we report a parametrization of the MM3(96) force field for metal complexes with aliphatic amide ligands in which the amide is coordinated to the metal ion through the oxygen donor atom. The ligands examined in this study are shown in Figure 1. The parametrization was accomplished by fitting to crystal structure data of fifty-two metal complexes. To obtain a model with broad applicability, we have considered all metal ions for which there were data available. These include members of the alkaline earths, transition metals, lanthanides, and actinides. A novel aspect of this study is the development of relationships between metal-dependent force field parameters and metal ion properties (charge, ionic radius, and electronegativity). These relationships yield a general model that can be applied to a wide range of metal ions.

2. Methods

2.1. Hardware and Software. Molecular mechanics calculations were carried out using the MM3(96) program.[22] The full-matrix minimization method was used where possible. The block diagonal minimization method with a reduced convergence criteria of 10^{-7} Å was used for structures with greater than 120 atoms and for uranyl complexes. The molecular graphics program, Chem 3D Plus[23] was used to visualize all downloaded crystal structures, to generate initial sets of molecular coordinates for MM3, and to plot the molecular structures obtained from energy minimization by the MM3 program.

2.2. Selection of Crystal Structures. The Cambridge Structural Database[24] was searched to locate metal−amide complex structures for use in the force field parametrization. Several structures were obtained from other sources.[25] Amide ligands were restricted to those (i) bearing either hydrogen or aliphatic substituents, (ii) that were coordinated to the metal ion through oxygen, and (iii) that did not contain other types of donor groups. There are few examples of metal complexes that contain only amide ligands. Therefore, other types of inner sphere ligands were permitted to enlarge the data set. These ligand types were restricted to H_2O, NO_3, Cl, NCS, and BH_3CN. Structures exceeding an upper limit for the *R* factor of 0.07 were discarded with few exceptions. Structures were also excluded for other reasons such as structural disorder or anomalous organic bond lengths. A total of 52 metal−amide complexes were selected for this study.[25]

2.3. Potential Functions. The MM3 program was originally designed to model organic compounds and transition metal complexes with common idealized metal geometries encountered at low coordination numbers, i.e., tetrahedral, square planar, trigonal bipyramidal, square pyramidal, and octahedral. Recently the program has been modified to allow its application to a wider range of metal ion geometries.[26] MM3(96) now supports a new type of metal atom type, which we will call a points-on-a-sphere (POS) metal.

A POS metal atom is treated like any normal atom except for the following features. The number of allowed attachments is increased to 20. All L−M−L bending interactions are removed and 1,3 van der Waals interactions are added between all donor atoms, L, connected to M. All M−L−X bending interactions are retained, but all stretch−bend and bend−bend terms that involve M are removed. Finally all L−M−L−X torsional interactions, typically omitted from MM calculations on metal complexes, are removed.

(15) (a) Hay, B. P. *Coord. Chem. Rev.* **1993**, *126*, 177−236. (b) Hay, B. P.; Clement, O. In *The Encyclopedia of Computational Chemistry*; Schleyer, P. v. R., Ed.; John Wiley and Sons: London, in press.
(16) Pozigun, D. V.; Kuz'min, V. E.; Kamalov, G. L. *Russ. Chem. Rev.* **1990**, *59*, 1093−1105.
(17) Timofeeva, T. V.; Struchkov, Y. T. *Russ. Chem. Rev.* **1990**, *59*, 320−343.
(18) Comba, P.; Hambley, T. W. *Molecular Modeling of Inorganic Compounds*; VCH: New York, 1995.
(19) Landis, C. R.; Root, D. M.; Cleveland, T. *Reviews in Computational Chemistry*; VCH: New York, 1995; Vol. 6.
(20) Zimmer, M. *Chem. Rev.* **1995**, *95*, 2629−2649.
(21) Hay, B. P. *Recent Advances in Metal Ion Separation and Pretreatment*; Rodgers, R. D., Bond, A. H., Dietz, M. L., Eds.; ACS Symposium Series; American Chemical Society: Washington, DC, in press.
(22) The calculations described herein were carried out with MM3(96). The program may be obtained from Tripos Associates, S.H.R., St. Louis, MO 63144, for commercial users, and it may be obtained from the Quantum Chemistry Program Exchange, Mr. Richard Counts, QCPE, Indiana University, Bloomington, IN 47405, for noncommercial users.
(23) Chem 3D software is available from CambridgeSoft Corporation, M.A., Cambridge, MA 02139, USA.
(24) Allen, F. H.; Bellard, S. A.; Brice, M. D.; Cartwright, B. A.; Doubleday: A.; Higgs, H.; Hummelink, T.; Hummelink-Peters, B. G.; Kennard, O.; Motherwell, W. D. S.; Rodgers, J. R.; Watson, D. G. *Acta Crystallogr. B* **1979**, *35*, 2331.
(25) (a) Cambridge Structural Database reference codes for these structures are as follows: DURSAK (**1**); NMALIE (**2**); TOFKUU (**3**); YEMNOT (**4**); COBHIK (**5**); JUWJUG (**6**); ZOWKAX (**7**); MALCDB (**8**); CIPCOT (**9**); GAZGET (**10**); VAMFIY (**11**); DMFAFE (**12**); WEHGEV (**13**); JAFFAX (**14**); ZUZPEP (**15**); DIYYAL (**16**); DIYXUE (**17**); MALCDA (**18**); ZACHUG (**19**); TABCAA (**20**); BAKHUQ (**21**); WEXMOB (**23**, **24**); TAQZIU (**32**); VOTKUK (**33**); CIDJIU (**34**); CIDKAB (**38**, **39**); SMFPHB (**40**); WADMIX (**42**); WADMOD (**43**); COJPAS (**44**); BECVAG (**45**); BIFLOR (**46**); CAHCET (**47**); BOHMUG (**48**); FEPFAH (**49**, **50**); HALFUV (**51**); HEPGEO (**52**). (b) Structural data for **22**, **25**−**28**, **30**, **31**, **35**−**37**, and **41**, were provided by Dr Brian M. Rapko, Pacific Northwest National Laboratory, Richland, WA, and Dr. Robin D. Rogers, Department of Chemistry, University of Alabama, Tuscaloosa, AL. (c) Structural data for **29** was provided by Dr. Michael G. B. Drew, Department of Chemistry, University of Reading, Berkshire, U.K.
(26) Hay, B. P.; Yang, L.; Lii, J.-H.; Allinger, N. L. *J. Mol. Struct. (THEOCHEM)* **1998**, *428*, 203−219.

This new feature greatly expands the potential for application of the MM3 program to coordination compounds. Advantages of the POS method are (i) with little to no modification, the default MM3 model can be applied to the ligand portion of the metal complexes, (ii) the explicit definition of M−L, M−L−X, and M−L−X−X interactions allows the interpretation of steric effects in terms of optimal bond lengths, bond angles, and torsion angles, and (iii) it accurately yields the geometries found about high-coordinate metal centers such as those encountered in complexes of the alkali, alkaline earth, lanthanide, and actinide metal ions.[15] With only one exception, we have used the new POS metal atom type to model all of the types of metal centers examined in this study (a representative structure input file and parameter file are provided as Supporting Information).

The exception arises with uranyl complexes **48**−**52** that all contain two oxo groups, two bidentate nitrates, and two amide ligands. The POS method fails to reproduce the ∼180° O═U═O and ∼90° O═U−$O_{nitrate}$ angles present in these complexes. Therefore, an alternate treatment was adopted. A $UO_2(NO_3)_2$ complex was constructed using normal MM3 atom types such that we could impose preferences for a O═U═O angle of 180° and O═U−$O_{nitrate}$ angles of 90°. The two amide oxygens were attached to a POS metal atom and the POS metal atom was superimposed on the metal center of the $UO_2(NO_3)_2$ complex. This gave a model in which the amide ligands were free to adopt any O_{amide}−U−$O_{nitrate}$ and O_{amide}−U═O angles with respect to the constrained $UO_2(NO_3)_2$ geometry (a structure input file and parameter file for a uranyl complex are provided as Supporting Information).

2.4. Metal-Independent Amide Parameters. As in other applications of molecular mechanics to coordination compounds,[15] we adopt the assumption that the majority of the force field parameters used for modeling the various interactions in metal-free amides are transferable to the amide portion of a metal complex. Moreover, we assume that these parameters are independent of the identity of the metal ion.[15,18] A recent review of the structural aspects of metal−amide complexes fully supports these assumptions.[11] It was found that the coordination of any metal ion to the amide oxygen resulted in only minor changes to the C═O and Csp^2−Nsp^2 bond lengths and caused no observable change to amide bond angles and torsion angles.

In this application of MM3, the term metal-independent refers to the parameters used for interactions that involve the amide carbon (atom type 3), the amide nitrogen (atom type 9), the amide oxygen (atom type 7), the sp^3 carbon (atom type 1), and hydrogens attached to carbon (atom type 5) or nitrogen (atom type 28). With the few exceptions, detailed below, the default MM3 parameters (1996 version) were applied to all interactions involving the aforementioned atom types. The modified MM3 amide parameter set (see Table 1) reproduced the structural features of metal-coordinated amide ligands examined in this study to within ±0.02 Å for bond lengths, 3° for bond angles, and 10° for torsion angles.

The default MM3 model uses several dielectric dependent parameters to account for changes in amide structure that occur on going from gas phase to condensed phase.[27] These changes include an increased C═O length, a decreased Csp^2−Nsp^2 length, and an increase in the barrier to rotation about the Csp^2−Nsp^2 bond. Complexation of a metal ion causes the C═O bond length to increase from 1.22 to 1.24 Å and the Csp^2−Nsp^2 bond length to decrease from 1.34 to 1.32 Å, on average.[11] In this study, we have used the default MM3 gas-phase dielectric constant of 1.5 and adjusted the strain-free C═O and Csp^2−Nsp^2 bond lengths to account for these changes (see Table 1).

Table 1. Modifications to the Default MM3(96) Parameter Set[a]

stretch	k_r (mdyn Å^{-1})	r_0 (Å)
3−7[b]	10.100	1.223
3−9	6.700	1.331
bend	k_θ (mdyn Å rad^{-2})	θ_0 (deg)
3−1−3	0.700	107.0
torsion	V_1 (kcal mol^{-1})	V_2 (kcal mol^{-1})	V_3 (kcal mol^{-1})
1−1−3−9	−0.457	0.097	−0.630
5−1−3−9	0.000	0.000	−0.254
5−1−9−1	0.000	0.000	0.936
3−1−3−9	0.185	−2.296	0.923
1−3−9−1	1.100	6.270	0.000
5−3−9−1	1.000	6.435	0.000
7−3−9−1	−0.600	6.930	0.000
1−3−9−28	0.000	6.270	0.000
7−3−9−28	1.000	6.765	0.000

[a] Parameters are presented in standard MM3 format. MM3 atom type numbers are as follows: 1, Csp^3; 3, Csp^2; 5, hydrogen attached to carbon; 7, carbonyl oxygen; 9, amide nitrogen; 28, hydrogen attached to amide nitrogen. [b] The program adds a 0.010 Å bond length correction such that the applied r_0 value is actually 1.233 Å.

Torsional interaction terms for rotation about the Csp^2−Nsp^2 bond were set to the default high dielectric limit (see Table 1). This parameter change raises the rotation barrier with respect to the gas-phase value. For example, MM3 yields a gas-phase value of 14.3 kcal/mol and a condensed phase value of 18.6 kcal/mol for Csp^2−Nsp^2 bond rotation in formamide.[27] Although the complexation of a metal ion may result in further increases to this torsional barrier,[28,29] we have no structural basis for the assignment of modified Csp^2−Nsp^2 torsional parameters. In all cases examined, the experimental data shows that the amide group is essentially planar and the torsional parameters are of a sufficient magnitude to ensure that planarity is maintained during the calculations. Thus, we note that although the model correctly reproduces structure, it may yield a lower limit for the barrier for rotation about the Csp^2−Nsp^2 bond when a metal ion is coordinated to oxygen.

Other modifications to the default MM3 force field involve the reassignment of parameters for the Csp^2−Csp^3−Csp^2 bend found in malonamide derivatives and of torsional interactions for rotation about Csp^2−Csp^3 and Nsp^2−Csp^3 bonds as shown in Table 1. These modifications are based on geometries and potential energy surfaces calculated at the MP2 level of theory using polarized double-ζ basis sets for acetamide, propanamide, 2-methylpropanamide, and 2,2-dimethylpropanamide,[30] and malonamide, *N*,*N*′-dimethylmalonamide, and *N*,*N*,*N*′,*N*′-tetramethylmalonamide.[31]

2.5. Treatment of Non-Amide Ligands. Many of the metal complexes selected for parameter optimization contain other ligand types in addition to the amide ligands. We observed in prior work on macrocyclic ether complexes of the alkali and alkaline earth cations that the influence of such ancillary ligands could be modeled by simply including the donor atom of each non-ether ligand with fixed M−L lengths corresponding to the

(27) Lii, J.-H.; Allinger, N. L. *J. Comput. Chem.* **1991**, *12*, 186−189.
(28) Rode, B. M. In *Metal−Ligand Interactions in Organic Chemistry and Biochemistry, Part 1*; D. Reidel Publishing Co.: Dordrecht-Holland, 1977.
(29) Sigel, H.; Martin, R. B. *Chem. Rev.* **1982**, *82*, 385−426.
(30) Sandrone, G.; Dixon, D. A.; Hay, B. P. *J. Phys. Chem.*, submitted.
(31) Sandrone, G.; Dixon, D. A.; Hay, B. P., manuscript in preparation.

observed M−L lengths in crystal structures.[6,26] In the current study, however, we found it necessary to include the complete structure of the ancillary ligand in the calculations. The approach used was to assign a single set of metal-independent parameters to reproduce the intra-ligand structure and to assign differing metal-dependent parameters for each complex to constrain the distance and orientation with respect to the metal ion. This approach yields an inner coordination sphere containing nonamide ligands with average intraligand geometries at the experimental M−L distances and M−L−X angles. Because they are connected to a POS metal center, L−M−L angles are unconstrained and, with the exception of the uranyl complexes, all ancillary ligands are free to move on the surface of a sphere defined by their M−L length.

Metal-independent parameters were either taken from the literature (aquo and nitrato)[32] or else high force constants (15 mdyn Å^{-1} or 15 mdyn Å rad^{-2}) were used to constrain bond lengths and angles to their experimental average values (thiocyanate, cyanoborohydride, and oxo). Default MM3 van der Waals radii were used for all atom types except for the chloride anion where literature values (r = 2.61 Å and ϵ = 0.062 kcal mol^{-1})[33] were applied. Metal-dependent parameters for M−L stretches and M−L−X bends were constrained to their experimental average values by assigning high force constants. The M−L−X−X torsion parameters were either taken from the literature (nitrato)[32] or set to zero (thiocyanate and cyanoborohydride).

2.6. Metal-Dependent Amide Parameters. Only three additional interactions were used to model the interaction of the amide with a given metal type. These are the M−O stretch interaction that controls the distance between the metal center and the amide oxygen and the M−O═C bend and M−O═C−X (X = C, H, N) torsion interactions that control the orientation of the amide with respect to the metal center. Nonbonded interactions involving the metal, e.g., van der Waals and electrostatic, were intentionally disabled by setting the appropriate parameters to zero.[15]

Parameters were obtained by empirical fits to crystal structures of **1**−**52**. The fitting process was accomplished by applying the following procedure. First the M−O lengths and M−O═C angles were constrained to their average crystal values using high force constants and V_2 parameters for the M−O═C−X torsion were manually adjusted to obtain agreement with experiment. During this process the same V_2 value was used for the M−O═C−N and the M−O═C−X (X = C, H) interactions, i.e., the barrier to rotation about the C═O bond was equally divided between the two interactions. After V_2 parameters were assigned, the M−O═C bending parameters, θ_0 and k_θ, were manually adjusted to obtain agreement with experiment. Finally, after θ_0 and k_θ were assigned, the M−O stretching parameters, r_0 and k_r, were adjusted to obtain agreement with experiment.

This procedure does not yield a unique set of parameters for any one complex. Instead we obtained ranges of r_0 and k_r combinations, θ_0 and k_θ combinations, and V_2 values that yielded similar levels of agreement with experiment. It was possible to identify a narrower range of transferable parameters when more than one complex was available for a given metal ion type. Relationships between these parameters and metal ion properties such as ionic radius, charge, and electronegativity were developed and used to calculate the final set of metal-dependent amide parameters shown in Table 2.

III. Results and Discussion

1. Relationships between MM3 Parameters and Metal Ion Properties. It is expected that the metal-dependent parameters used in molecular mechanics models should vary as a function of metal ion properties. Examples of this behavior were observed during the parametrization of an extended MM3 force field for ether complexes with the alkali and alkaline earth cations.[6,26] In this model the k_r values for the M−O stretches, the k_θ values for the M−O−C bends, and the V_i values for the M−O−C−X torsions correlated with the size and charge of the metal ion. The parameters vary so that distortions from the preferred geometries become easier as the M−O distance increases and as the metal ion charge decreases.

Relationships with metal ion properties have been used in other force field parametrizations for a given ligand with a variety of metal ions. Empirical rules and relationships have been used to obtain r_0 and k_r values for M−L stretches in the MMX,[34] DREIDING,[35] and UFF [36] force fields. The UFF and DREIDING force fields assign a metal invariant θ_0 value for M−L−X angles. The UFF force field generates M−L−X bending force constants using an angular generalization of Badger's rules whereas the DREIDING force field uses a metal invariant bending force constant. Both the UFF and DREIDING force fields employ metal invariant parameters for M−L−X−X torsions. Details on the assignment of the parameters associated with M−L−X bends and M−L−X−X torsions in the MMX force field were not presented.[34]

In this study, we have examined metal-dependent amide parameter sets for 22 metal ions and find that all five metal-dependent amide parameters vary as physical properties of the metal ion change. In what follows, we report the first example of a force field for an entire class of metal complexes in which all of the metal-dependent parameters are derived from empirical relationships with metal ion properties.

M−O Stretch. The r_0 parameter is given in units of Å by eq 1 where IR is the Shannon ionic radius associated with the effective coordination number of the metal ion.

$$r_0 = 1.049(\mathrm{IR}) + 1.143 \qquad (1)$$

These radii are available for the common coordination numbers of most metal ions.[37] The effective coordination number is obtained by assigning a contribution of 1.5 from the two oxygen donors of the bidentate nitrate ligand. This treatment leads to fractional coordination numbers. In such cases, the ionic radii were estimated from plots of ionic radius versus coordination number. Effective coordination numbers, Shannon ionic radii, and r_0 values for the metal complexes examined in this study are given in Table 2.

The k_r parameter is given in units of mdyn Å^{-1} by eq 2

$$k_r = 0.199Z/\mathrm{IR} \qquad (2)$$

where Z is the formal charge of the metal ion and IR is the Shannon ionic radius as defined above. This functional form

(32) Hay, B. P. *Inorg. Chem.* **1991**, *30*, 2876−2884.
(33) Peng, Z.; Ewig, C. S.; Hwang, M.-J.; Waldman, M.; Hagler, A. T. *J. Phys. Chem. A* **1997**, *101*, 7243−7252.
(34) Gajewski, J. J.; Gilbert, K. E.; McKelvey, J. In *Advances in Molecular Modelling*; JAI Press: Greenwich, CT, 1990; Vol. 2.
(35) Mayo, S. L.; Olafson, B. D.; Goddard, W. A., III. *J. Phys. Chem.* **1990**, *94*, 8897−8909.
(36) Rappe, A. K.; Colwell, K. S.; Casewit, C. J. *Inorg. Chem.* **1993**, *32*, 3438−3450.
(37) Shannon, R. D. *Acta Crystallogr. A* **1976**, *32*, 751−767.

Table 2. Metal Properties and MM3 Metal-Dependent Amide Parameters[a]

	complex	CN	IR (Å)	EN	IC	r_0 (Å)	k_r (mdyn Å^{-1})	θ_0 (deg)	k_θ (mdyn Å rad^{-2})	V_2 (kcal mol^{-1})
1	$[Mg(NMA)_2(OH_2)_4]^{2+}$	6	0.72	1.31	0.673	1.898	0.553	135.1	0.061	0.289
2	$[Mg(NMA)_6]^{2+}$	6								
3	$[Mg(DMF)_4(OH_2)_2]^{2+}$	6								
4	$[Mg(DMA)_6]^{2+}$	6								
5	$[Ca(DMF)_2(OH_2)_2Cl_2]$	6	1.00	1.00	0.780	2.192	0.398	140.5	0.038	0.139
6	$[Ca(DMF)_6]^{2+}$	6								
7	$[Ca(DMA)_3Cl_3]^-$	6								
8	$[Mn(MAL)_2(O-NO_2)_2]$	6	0.83	1.55	0.583	2.014	0.480	130.9	0.091	0.519
9	$[Fe(DMF)_6]^{2+}$	6	0.78	1.83	0.470	1.961	0.510	126.6	0.151	0.921
10	$[Fe(DMF)_6]^{2+}$	6								
11	$[Fe(DMF)_6]^{2+}$	6								
12	$[Fe(DMF)_6]^{3+}$	6	0.645	1.96	0.414	1.820	0.926	129.1	0.194	0.655
13	$[Fe(DMF)_5Cl]^{2+}$	6								
14	$[Co(DMF)_4(NCBH_3)_2]$	6	0.745	1.88	0.449	1.925	0.534	126.0	0.166	1.013
15	$[Ni(DMF)_6]^{2+}$	6	0.69	1.91	0.436	1.867	0.577	125.6	0.176	1.055
16	$[Zn(MAL)_2(O-NO_2)_2]$	6	0.74	1.65	0.544	1.919	0.538	129.2	0.109	0.646
17	$[Zn(MAL)_2(NCS)_2]$	6								
18	$[Cd(MAL)_2Cl_2]$	6	0.95	1.69	0.528	2.140	0.419	128.6	0.117	0.701
19	$[Cd(BOPA)_2(NO_3)_2(OH_2)]$	6								
20	$[Zr(DMF)_2Cl_4]$	6	0.72	1.51[b]	0.599	1.898	1.106	143.9	0.085	0.088
21	$[La(TMMA)_5]^{3+}$	9	1.216	1.10	0.747	2.419	0.491	144.8	0.044	0.077
22	$[La(TMMA)_2(NO_3)_3]$	8.5	1.186			2.387	0.503			
23	$[La(TEMA)_2(NO_3)_3]$	8.5	1.186							
24	$[La(TEMA)_2(NO_3)_3]$	8.5	1.186							
25	$[La(TMSA)_3(NO_3)_3]^{3+}$	8.5	1.186							
26	$[Ce_2(TMSA)_3(NO_3)_6]$	7.5	1.108	1.12	0.740	2.305	0.539	144.5	0.046	0.080
27	$[Pr_2(TMSA)_3(NO_3)_6]$	7.5	1.088	1.13	0.736	2.284	0.549	144.3	0.046	0.083
28	$[Nd(TMMA)_2(NO_3)_3]$	8.5	1.135	1.14	0.733	2.334	0.526	144.2	0.047	0.084
29	$[Nd(DCMMA)_2(NO_3)_3]$	8.5	1.135							
30	$[Nd_2(TMSA)_3(NO_3)_6]$	7.5	1.075			2.270	0.555			
31	$[Nd(TMSA)_4]^{3+}$	8	1.09			2.286	0.548			
32	$[Nd(DMF)_8]^{3+}$	8	1.09							
33	$[Nd(\Delta\text{-}VAM)_8]^{3+}$	8	1.09							
34	$[Sm(DMA)_3(NO_3)_3]$	7.5	1.05	1.17	0.723	2.244	0.569	143.8	0.049	0.090
35	$[Eu(TMSA)_4]^{3+}$	8	1.066	1.19	0.716	2.261	0.560	143.5	0.051	0.093
36	$[Gd(TMMA)_2(NO_3)_3]$	8.5	1.08	1.20	0.712	2.276	0.553	143.3	0.051	0.095
37	$[Gd_2(TMSA)_3(NO_3)_6]$	7.5	1.028			2.221	0.581			
38	$[Er(DMA)_3(NO_3)_3]$	7.5	0.977	1.24	0.698	2.168	0.611	142.6	0.055	0.104
39	$[Er(DMA)_3(NO_3)_3]$	7.5	0.977							
40	$[Er(TMMA)_4]^{3+}$	8	1.004			2.196	0.595			
41	$[Yb_2(TMSA)_3(NO_3)_6]$	7.5	0.955	1.26	0.691	2.145	0.625	142.3	0.057	0.108
42	$[Th(DCHA)_3(NCS)_4]$	7	0.99	1.45[b]	0.622	2.182	0.804	144.8	0.077	0.077
43	$[Th(D^iPPA)_3(NCS)_4]$	7								
44	$[U(D^iPA)_4(NCS)_4]$	8	1.00			2.192	0.796	146.0	0.067	0.066
45	$[U(DM^iPA)_3(NCS)_4]$	7	0.95	1.37[b]	0.651	2.140	0.838			
46	$[U(DEPA)Cl_5]^-$	6	0.89			2.077	0.894			
47	$[U(DM^tBA)_2Cl_4]$	6	0.89							
48	$[UO_2(DMF)_2(NO_3)_2]$	7	1.055[b]	na	na	2.250	0.377	143.0[c]	0.05[c]	0.099
49	$[UO_2(DBNPA)_2(NO_3)_2]$	7								
50	$[UO_2(DBNPA)_2(NO_3)_2]$	7								
51	$[UO_2(\Delta\text{-}VAM)_2(NO_3)_2]$	7								
52	$[UO_2(TBSA)(NO_3)_2]$	7								

[a] CN = effective coordination number as defined in text. IR = Shannon ionic radius.[37] EN = electronegativity (from a table of Pauling electronegativies in Huheey, J. E. *Inorganic Chemistry: Principles of Structure and Reactivity*, 1978). IC = ionic character as defined by Pauling.[40] Parameters are presented in standard MM3 format for the M−O stretch (from eqs 1 and 2), the M−O=C bend (from eqs 3 and 4), and the M−O=C−X torsion (from eq 5). [b] Assumed value. [c] In the absence of an EN value for the UO_2^{2+} ion, bending parameters for the uranyl ion were assigned by comparison to other f-block metals.

exhibits the expected behavior of increasing force constant with increasing charge and decreasing distance. In addition, it yields the correct asymptotic limit of a zero force constant at infinite separation. The k_r values for the metal complexes examined in this study are given in Table 2.

We also explored the possibility of using other empirical relationships to obtain the stretching force constants. Badger's relationship[38,39] has successfully correlated bond stretching force constants as a function of bond length in a variety of diatomic molecules. In the current model, application of Badger's relation with experimentally observed M−O bond lengths generally gave higher k_r values than eq 2 and we were unable to derive a corresponding set of r_0 values such that the r_0 values could be linearly correlated with Shannon's ionic radii (eq 1).

M−O−C Bend. Significant differences in M−O−C angular preference exist between the predominantly ionic (alkaline earth, lanthanides, and actinides) and the more covalent metals (first-row transition metals).[11] Therefore, it was not possible to assign a single θ_0 value for all metal ions. An alternate approach is to

(38) Badger, R. M. *J. Chem. Phys.* **1935**, *3*, 710−714.

(39) Herschbach, D. R.; Laurie, V. W. *J. Chem. Phys.* **1961**, *35*, 458−463.

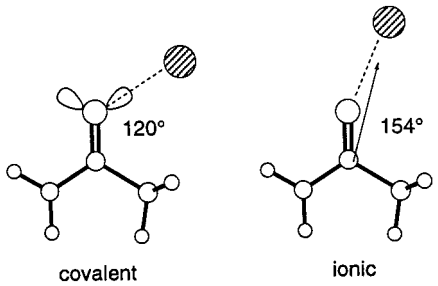

Figure 2. Predicted M−O═C angles based on ideal geometries for a pure covalent interaction (left) and a pure ionic interaction (right). Arrow on the right shows the orientation of the acetamide dipole moment (MM3).

compute a value of θ_0 for each metal. The θ_0 parameter is given in units of degrees by eq 3

$$\theta_0 = 137.4 + 17.6 \tanh(2.886\mathrm{IC} + 0.364Z - 2.800) \quad (3)$$

where Z is the formal charge of the metal ion and IC is the ionic character of the M−O bond derived from differences in electronegativity of oxygen and the metal.[40] Electronegativities, IC values, and θ_0 values are given in Table 2 for the metal ions examined in this study.

The hyperbolic tangent function in eq 3 asymptotically approaches a limit of 120.1° ($Z = 1$) as the ionic character of the M−O bond goes to zero and limit of 153.4° ($Z = 4$) as the ionic character of the M−O bond goes to 100%. These limiting behaviors can be rationalized in terms of expected ideal geometries for a pure covalent or a pure ionic interaction as illustrated in Figure 2. In the idealized covalent case, optimal overlap between a metal centered orbital with an sp^2 oxygen orbital occurs at an M−O═C angle near 120°. In the idealized ionic case, the optimal interaction occurs when the metal aligns with the dipole moment of the ligand. Alignment of the metal ion with the dipole moment of acetamide predicts a M−O═C angle 154° at an M−O distance of 2.5 Å.

The k_θ parameter is given in units of mdyn Å rad^{-2} by eq 4

$$k_\theta = 1.219 \exp(-4.443IC) \quad (4)$$

where IC is the ionic character of the M−O bond as described above. This exponential relationship yields k_θ limits ranging from 1.22 mdyn Å rad^{-2} for a pure covalent M−O bond to 0.014 mdyn Å rad^{-2} for a pure ionic M−O bond. The former value is of the same magnitude as bending force constants found in the MM3 force field for bends that occur in organic molecules, e.g., the C(sp^3)−C(sp^3)−C(sp^3) bend interaction has a k_θ of 0.67 mdyn Å rad^{-2}. The k_θ values for the metal complexes examined in this study are given in Table 2.

M−O═C−X Torsions. Rotation about the C═O bond of a coordinated amide is defined by two dihedral angles. These are the M−O═C−N angle and the M−O═C−X angle (X = C, H). A 2-fold torsional potential is used to reproduce the preference for the metal ion to lie in the plane of the amide[11] and the same V_2 parameter is used for both interactions. The V_2 parameter is given in units of kcal mol^{-1} by eq 5

$$V_2 = 2.835 \times 10^7 \exp(-0.1362\theta_0) \quad (5)$$

where θ_0 is the ideal M−O−C angle as obtained from eq 3. This exponential function yields higher M−O═C−X rotational barriers for the more covalent metals (smaller θ_0) and lower rotational barriers for the more ionic metals (larger θ_0). The V_2 values for the metal complexes examined in this study are given in Table 2.

2. Model Performance. Starting from their crystal structure coordinates, structures **1**−**52** were calculated with the extended MM3 model described above. A detailed comparison of experimental and calculated structural features was performed. The results of this comparison are summarized in Table 3. Structures are grouped by metal ion type. For each complex we report (i) calculated average values, experimental average values, and the mean absolute deviations in M−O_{amide} distances, M−O═C angles, and M−O═C−X torsion angles, (ii) the mean absolute deviation in all L−M−L angles, and (iii) the root-mean-squared deviation (rmsd) between the calculated and experimental atom positions for all non-hydrogen atoms. When more than one complex is present per metal ion, we also report the average performance in each column as well as the experimental range of values for the M−O_{amide} distances, M−O═C angles, and M−O═C−X torsion angles.

The average mean absolute deviation for M−O_{amide} distances in **1**−**52** is 0.038 Å. The extent of the deviation correlates with the experimental range of M−O distance. Individual first-row transition metals exhibit M−O_{amide} distance ranges of 0.05−0.08 Å and in these cases the model gives a mean absolute deviation of 0.022 Å. The more ionic metals exhibit M−O_{amide} distance ranges of up to 0.17 Å and in these cases the model gives a mean absolute deviation of 0.042 Å. For any given metal ion the mean absolute deviation in M−O_{amide} distance is less than the experimental range of values indicating that the model is accounting for the variability in M−O_{amide} distance.

The average mean absolute deviation for M−O═C angles in **1**−**52** is 4.1°. This value is quite good given the wide range of M−O═C angles observed within each metal type. For individual metal ions the mean absolute deviations are typically five times less than the experimental ranges. The average mean absolute deviation for L−M−L angles (L = O, N, Cl) in **1**−**52** is 3.3°. This level of agreement demonstrates the POS method of treating metal-centered angles to be accurate and of sufficient flexibility to accommodate the wide range of coordination geometries encountered in the 6- to 9-coordinate metal−amide complexes examined in this study.

The average mean absolute deviation for M−O═C−X dihedral angles in **1**−**52** is 10.2°. Although somewhat larger than obtained in previous applications of this type of model (±5−6°),[6,26,41] this value is acceptable given the wide range of M−O−C−X dihedral angles observed within each metal type and the possible influence of crystal packing effects. The majority of the amide ligands examined in this study are connected to the metal ion by a single M−O bond whereas the previous studies have focused on multidentate ligands in which there are additional intra-ligand constraints on the M−L−X−X dihedral angles. When coupled with the low barriers to rotation, a single point of attachment to the metal ion renders the M−O═C−X dihedral angles in the amide complexes more susceptible to distortions caused by intermolecular interactions that may be present in the crystal lattice.

The average root-mean-squared deviation (rmsd) between the calculated and experimental atom positions for all non-hydrogen atoms in **1**−**52** is 0.326 Å. After examination of overlays of

(40) Pauling, L. *The Nature of the Chemical Bond*; Cornell University Press: New York, 1960.

(41) Cundari, T. R.; Moody, E. W.; Sommerer, O. *Inorg. Chem.* **1995**, *34*, 5989−5999.

Table 3. Comparison of Calculated versus Experimental Structural Features[a]

		M−O_{amide}			M−O═C			M−O═C−N			L−M−L	
complex		calc (exp)	dev	range	calc (exp)	dev	range	calc (exp)	dev	range	dev	rmsd
Mg^{2+}	**1**	2.101 (2.046)	0.055		143.6 (141.8)	1.8		153.2 (161.4)	8.2		1.8	0.098
	2	2.099 (2.064)	0.035		138.9 (142.3)	4.1		148.1 (152.4)	8.1		1.2	0.299
	3	2.105 (2.058)	0.047		126.9 (129.9)	5.3		176.6 (177.1)	1.2		3.9	0.548
	4	2.099 (2.059)	0.040		146.8 (147.3)	1.6		177.0 (171.0)	5.8		2.3	0.242
	av	*2.101 (2.058)*	*0.044*	*0.073*	*139.0 (140.3)*	*3.2*	*34.2*	*163 (165)*	*5.8*	*76*	*2.3*	*0.296*
Ca^{2+}	**5**	2.286 (2.342)	0.056		127.5 (128.0)	0.5		173.8 (176.6)	2.8		3.1	0.371
	6	2.306 (2.292)	0.049		136.7 (143.1)	6.9		108.4 (135.7)	23.4		3.6	0.403
	7	2.318 (2.297)	0.021		152.9 (161.2)	9.8		123.3 (148.1)	24.9		4.6	0.300
	av	*2.303 (2.310)*	*0.042*	*0.087*	*139.0 (143.7)*	*5.7*	*38.5*	*135 (154)*	*17.0*	*97*	*3.8*	*0.358*
Mn^{2+}	**8**	2.128 (2.124)	0.013		122.0 (125.5)	3.5		146.4 (153.9)	7.6		3.2	0.272
Fe^{2+}	**9**	2.134 (2.122)	0.019		122.7 (124.3)	2.8		173.3 (165.5)	7.8		2.2	0.549
	10	2.133 (2.095)	0.039		122.8 (126.0)	6.1		178.4 (176.4)	6.9		1.4	0.544
	11	2.134 (2.110)	0.024		122.8 (122.2)	4.4		179.7 (176.0)	3.9		1.2	0.434
	av	*2.134 (2.109)*	*0.027*	*0.077*	*122.8 (124.1)*	*4.4*	*17.6*	*177 (173)*	*6.2*	*27*	*1.6*	*0.509*
Fe^{3+}	**12**	1.983 (1.990)	0.007		129.0 (127.1)	2.6		176.5 (166.9)	13.7		1.3	0.507
	13	2.004 (2.019)	0.021		133.2 (128.1)	6.5		173.9 (178.0)	4.1		1.7	0.291
	av	*1.993 (2.004)*	*0.014*	*0.049*	*131.1 (127.6)*	*4.6*	*8.1*	*175 (172)*	*8.9*	*21*	*1.5*	*0.396*
Co^{2+}	**14**	2.062 (2.105)	0.043		126.1 (125.9)	1.5		178.6 (176.5)	2.1		1.6	0.363
Ni^{2+}	**15**	2.073 (2.050)	0.023		123.7 (124.0)	4.4		179.8 (172.2)	7.6		1.2	0.489
Zn^{2+}	**16**	2.074 (2.047)	0.028		123.0 (124.1)	1.3		151.9 (157.5)	5.6		3.1	0.283
	17	2.100 (2.091)	0.010		122.4 (125.1)	2.7		154.5 (167.8)	13.4		1.6	0.266
	av	*2.087 (2.069)*	*0.019*	*0.068*	*122.7 (124.6)*	*2.0*	*2.7*	*153 (163)*	*9.5*	*17*	*2.4*	*0.275*
Cd^{2+}	**18**	2.300 (2.329)	0.029		123.5 (128.3)	4.8		152.7 (168.3)	15.7		4.9	0.307
	19	2.218 (2.291)	0.073		135.2 (136.6)	1.6		174.9 (174.6)	3.8		3.7	0.367
	av	*2.259 (2.310)*	*0.051*	*0.056*	*129.3 (132.4)*	*3.2*	*11.1*	*164 (172)*	*9.7*	*11*	*2.0*	*0.337*
Zr^{4+}	**20**	2.012 (2.052)	0.039		151.9 (149.8)	2.2		179.9 (163.7)	16.3		0.8	0.133
La^{3+}	**21**	2.599 (2.537)	0.064		134.1 (135.1)	4.4		138.2 (143.3)	7.4		5.3	0.328
	22	2.480 (2.502)	0.021		132.5 (132.9)	5.0		119.8 (123.7)	6.2		3.5	0.486
	23	2.457 (2.508)	0.051		132.0 (134.5)	5.7		130.6 (136.9)	7.1		4.4	0.374
	24	2.486 (2.553)	0.067		130.4 (128.2)	5.7		129.4 (128.0)	14.4		6.0	0.451
	25	2.491 (2.475)	0.051		149.6 (154.2)	4.9		125.3 (118.5)	13.3		3.5	0.306
	av	*2.502 (2.515)*	*0.051*	*0.163*	*135.7 (136.9)*	*5.1*	*42.8*	*129 (130)*	*9.7*	*71*	*4.5*	*0.389*
Ce^{3+}	**26**	2.355 (2.405)	0.051		144.2 (146.7)	2.5		111.3 (110.2)	5.1		3.6	0.257
Pr^{3+}	**27**	2.340 (2.390)	0.051		144.8 (146.7)	1.9		112.0 (110.0)	5.1		3.4	0.230
Nd^{3+}	**28**	2.417 (2.446)	0.029		134.6 (133.3)	4.1		122.8 (125.8)	5.5		5.6	0.488
	29	2.416 (2.486)	0.069		132.0 (129.1)	3.9		117.9 (122.2)	6.7		4.1	0.267
	30	2.332 (2.373)	0.045		145.0 (146.6)	2.0		112.7 (110.4)	3.9		3.4	0.255
	31	2.464 (2.426)	0.045		140.7 (144.4)	8.0		128.9 (134.6)	19.0		4.7	0.307
	32	2.440 (2.433)	0.035		133.8 (139.0)	9.6		141.1 (148.1)	17.2		4.5	0.581
	33	2.526 (2.452)	0.075		136.6 (145.3)	8.7		14.5 (12.5)	21.0		8.5	0.320
	av	*2.433 (2.436)*	*0.050*	*0.123*	*137.1 (139.6)*	*6.0*	*30.2*	*107 (109)*	*12.2*	*91*	*5.1*	*0.370*
Sm^{3+}	**34**	2.326 (2.315)	0.011		150.1 (148.8)	8.6		132.1 (136.6)	8.6		1.8	0.250
Eu^{3+}	**35**	2.443 (2.388)	0.055		142.2 (145.9)	7.6		130.1 (140.0)	16.6		4.3	0.261
Gd^{3+}	**36**	2.400 (2.389)	0.024		132.2 (132.5)	5.6		141.5 (139.0)	21.0		3.8	0.494
	37	2.286 (2.323)	0.045		142.6 (146.5)	2.3		111.8 (110.1)	6.7		3.9	0.283
	av	*2.343 (2.356)*	*0.034*	*0.096*	*137.4 (139.5)*	*3.9*	*26.9*	*127 (125)*	*13.8*	*72*	*3.8*	*0.389*
Er^{3+}	**38**	2.252 (2.257)	0.015		152.4 (152.7)	6.5		136.2 (143.3)	10.6		1.5	0.389
	39	2.263 (2.255)	0.035		155.2 (152.0)	3.2		150.6 (138.2)	13.8		1.5	0.273
	40	2.367 (2.312)	0.051		128.2 (133.2)	5.0		118.8 (138.8)	20.1		2.6	0.471
	av	*2.294 (2.275)*	*0.034*	*0.097*	*145.3 (146.0)*	*4.9*	*36.0*	*135 (140)*	*14.8*	*52*	*1.9*	*0.378*
Yb^{3+}	**41**	2.251 (2.250)	0.039		146.2 (146.4)	1.7		111.5 (111.2)	5.7		2.9	0.258
Th^{4+}	**42**	2.362 (2.357)	0.022		150.1 (151.9)	1.9		163.1 (151.1)	12.0		3.9	0.235
	43	2.301 (2.335)	0.034		165.6 (164.2)	1.1		120.2 (116.5)	9.7		3.3	0.154
	av	*2.332 (2.346)*	*0.028*	*0.030*	*157.8 (158.0)*	*1.5*	*12.4*	*142 (134)*	*10.8*	*64*	*3.6*	*0.195*
U^{4+}	**44**	2.390 (2.362)	0.027		146.2 (144.1)	2.1		115.5 (112.6)	2.9		1.0	0.136
	45	2.257 (2.304)	0.047		155.6 (158.6)	7.9		100.8 (100.2)	7.0		1.4	0.456
	46	2.185 (2.291)	0.106		164.4 (163.9)	0.5		168.8 (155.2)	13.6		2.7	0.255
	47	2.231 (2.247)	0.016		161.2 (165.2)	4.0		81.4 (90.6)	9.2		1.4	0.190
	av	*2.266 (2.301)*	*0.049*	*0.148*	*156.8 (157.9)*	*3.6*	*25.1*	*117 (115)*	*8.2*	*80*	*1.6*	*0.259*
UO_2^{2+}	**48**	2.348 (2.397)	0.049		141.6 (125.4)	16.2		168.1 (160.0)	8.1		1.4	0.236
	49	2.368 (2.358)	0.010		149.2 (154.2)	5.0		97.3 (111.0)	13.7		1.8	0.270
	50	2.417 (2.351)	0.066		138.7 (141.0)	2.3		97.5 (117.3)	19.8		1.6	0.282
	51	2.364 (2.359)	0.005		139.4 (142.6)	3.2		38.7 (27.9)	10.8		0.7	0.138
	52	2.400 (2.358)	0.042		135.1 (135.6)	0.8		109.2 (108.9)	3.7		2.4	0.214
	av	*2.386 (2.363)*	*0.034*	*0.074*	*140.8 (139.8)*	*5.5*	*28.8*	*102 (105)*	*11.2*	*132*	*1.6*	*0.228*

[a] Exp and calc are average values; dev is the mean absolute deviation computed by summing the deviations for all occurrences of the structural feature and dividing by the number of occurrences. Bond lengths and rmsd values in Å; bond angles and dihedral angles in deg.

calculated and experimental structures, we find that a rmsd of ≤0.3 Å indicates a very good fit. Twenty-eight of the structures examined meet this criterion. Figure 3 shows representative overlays from this group that highlight the accuracy to which this model reproduces a wide range of structurally diverse metal−amide complexes.

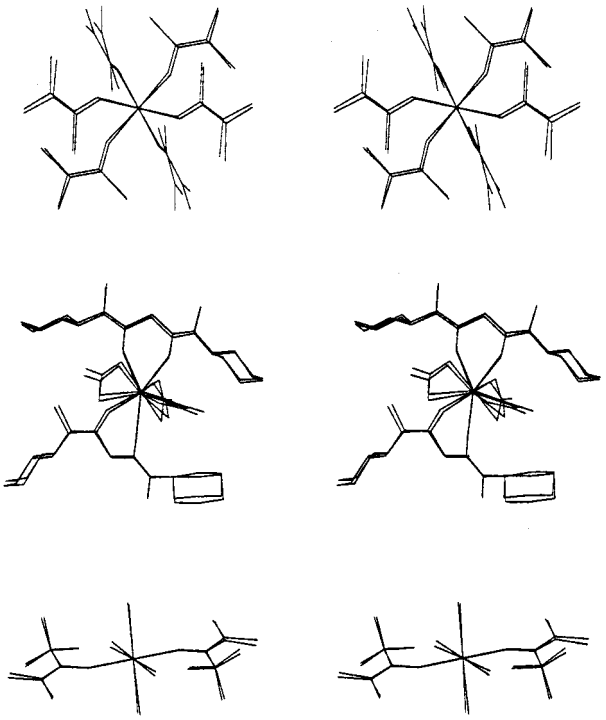

Figure 3. Overlays of experimental and calculated structures for **4** (rmsd = 0.242 Å), **29** (rmsd 0.267 Å), and **47** (rmsd = 0.190 Å).

Rmsd values in the range of 0.3−0.5 indicate a good to fair agreement with experiment. Nineteen structures meet this criterion. Figure 4 shows representative overlays from this group. In the case of **19**, where the model well reproduces both the inner sphere geometry and the amide orientation, the increased rmsd value is due to structural variations at the outer ends of the amide ligands. In the case of **36**, one of the malonamide ligands is well reproduced, but M−O−C−X torsional angle differences in the other malonamide ligand result in the higher rmsd value. Rmsd values ≥0.5 indicate fair-to-poor agreement with experiment. Only five structures are in this category. An overlay for the structure with the highest rmsd, **32** with 0.581 Å, is shown at the bottom of Figure 4. Here the large rmsd is primarily caused by the failure of the model to reproduce the experimental M−O−C−X torsion angles.

IV. Summary

We have developed an extended MM3(96) force field for metal amide complexes by fitting to crystal structure data. This model is based on a POS metal approach that requires the parametrization of only three metal-dependent interactions for a given metal ion; the M−O stretch, the M−O═C bend, and the M−O═C−X torsion. These interactions require the definition of five parameters per metal ion. A set of empirical relationships are used to generate these parameters as a function of metal ion size, charge, and electronegativity. The resulting model provides the first example of a force field in which all metal-dependent parameters are derived from metal ion properties.

The accuracy of the model was assessed by comparison of calculated and experimental structures. The overall mean absolute deviations between theory and experimental structural features are 0.038 Å for M−O distance, 4.1° for M−O═C angle, 3.3° for L−M−L angle, and 10° for M−O═C−X dihedral angle. This level of performance is comparable to that obtained with force fields for other ligand types with alkali and alkaline earth metals,[6,26] lanthanides,[32,41] and technetium(V).[42]

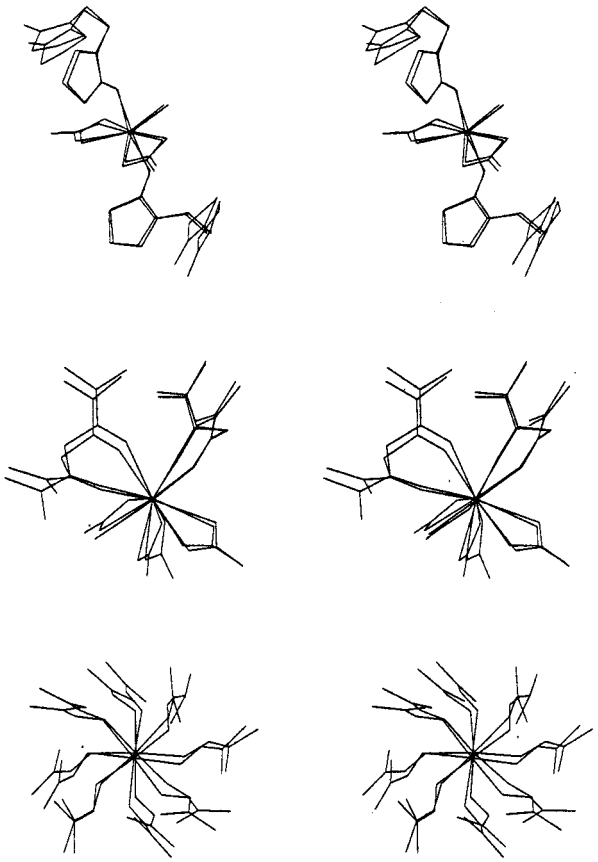

Figure 4. Overlays of experimental and calculated structures for **19** (rmsd = 0.367 Å), **36** (rmsd = 0.494 Å), and **32** (rmsd = 0.581 Å).

If the data is restricted to the 10 first-row transition metal complexes, in which there is less variation in the structural features, we obtain mean absolute deviations of 0.022 Å for M−O, 3.5° for M−O═C angle, 1.9° for L−M−L angle, and 7° for M−O═C−X dihedral angle. This level of performance is comparable to that obtained with force fields for other ligand types with the first row transition metal ions.[18,43−45]

Acknowledgment. Funding for this work was provided by the Environmental Management Science Program under direction of the U.S. Department of Energy's Office of Basic Sciences (ER-14), Office of Energy Research and the Office of Science and Technology (EM-52), Office of Environmental Management. Pacific Northwest National Laboratory is operated for the U.S. Department of Energy by Battelle Memorial Institute under Contract DE-AC06-76RLO 1830.

Supporting Information Available: MM3(96) structure input files and parameter files for $[Zn(MAL)_2(NCS)_2]$ and $[UO_2(TBSA)_2(NO_3)_2]$ (6 pages). Ordering information is given on any current masthead page.

IC980641J

(42) Hancock, R. D.; Reichert, D. E.; Welch, M. J. *Inorg. Chem.* **1996**, *35*, 2165−2166.
(43) Adam, K. R.; Antolovich, M.; Brigden, L. G.; Lindoy, L. F. *J. Am. Chem. Soc.* **1991**, *113*, 3346−3351.
(44) Bernhardt, P. V.; Comba, P. *Inorg. Chem.* **1992**, *31*, 2638−2644.
(45) Deeth, R. J.; Paget, V. J. *J. Chem. Soc., Dalton Trans.* **1997**, 537−546.